NUMERICAL MODELLING OF TIME-HARMONIC SEISMIC WAVE FIELDS IN SIMPLE STRUCTURES BY THE GAUSSIAN BEAM METHOD. PART II.

JANA KONOPÁSKOVÁ

Geophysical Institute, Czechosl. Acad. Sci., Prague)*

VLASTISLAV ČERVENÝ

*Institute of Geophysics, Charles University, Prague**)*

Резюме: *Эта работа является продолжением работы* [1]. *В обеих работах, метод гауссовских пучков используется для вычисления гармонических волн отраженных от плоской границы раздела. Главное внимание уделяется отраженным волнам типа PP. Сравнением с точными результатами было получено в* [1], *что метод гауссовских пучков дает достаточно точные результаты даже в сингулярной области начальной точки. В закритической области, суммированием гауссовских пучков отраженных волн получились даже головные волны. В этой работе обсуждается чувствительность результатов к разным параметрам расчетов, особенно к начальной ширине L_0 гауссовских пучков. Показано, что в регулярных лучевых областьях результаты практически не зависят от L_0. В области начальной точки и в закритической области, самые точные результаты получены для больших L_0. При уменьшении L_0, амплитуды отраженных волн в области начальной точки немножко понижаются, но положение максимума получается точно, от изменения L_0 не зависит. В закритической области, уменьшение L_0 имеет некоторый сгляживающий эффект на осциляции амплитудной кривой, соответствующие головным волнам. Для низких L_0, осциляции не получаются. Детально изучается чувствительность результатов даже к другим параметрам расчетов. Внимание уделяется также амплитудным кривым отраженных волн типа PS, SP и SS.*

1. INTRODUCTION

In [1], the method of Gaussian beams was used to compute the time-harmonic waves reflected from a plane interface between two homogeneous half-spaces. The purpose of these computations was to test the accuracy of the Gaussian beam method by comparing its results with those of exact solutions.

It was shown in [1] that, in this case, the method of Gaussian beams yields satisfactory results not only in the regular-ray regions, but also in the critical region, which is singular from the point of view of the ray method. In both regions, the method of Gaussian beams yields the results predicted by exact methods. Moreover, in the overcritical region, head waves were automatically obtained by superimposing reflected Gaussian beams.

Gaussian beam computations, however, are influenced by certain auxiliary computation parameters. The most important of them are the initial parameters of the Gaussian beams (such

*) Address: Boční II, 141 31 Praha 4-Spořilov.

**) Address: Ke Karlovu 3, 121 16 Praha 2.

as the initial halfwidth of the beam and initial curvature of the phase front of the beam), followed by the parameters of the expansion of the wave field into Gaussian beams, etc. In [1], the comparison of the results obtained by the Gaussian beam method with the exact solutions was presented only for one particular group of these parameters. It is, therefore, necessary to investigate the sensitivity of the results obtained by the method of Gaussian beams to these computation parameters.

This paper is a continuation of [1] which will be referred to as Paper I. The main aim of this paper is to investigate the influence of the computation parameters on the amplitude-distance curves of *PP* waves reflected from a plane interface. It will be shown that the results are generally stable with respect to these parameters. Only the initial width of the Gaussian beam has a certain smoothing influence on the amplitudes of reflected waves in the critical and overcritical regions. For comparison with the amplitude-distance curves of *PP* reflected waves, also other types of reflected waves are considered in Sec. 6, particularly the converted *PS* and *SP* reflected waves, and the *SS* reflected waves. The main conclusions drawn from our investigations are listed in Sec. 7.

We shall again consider the same model of the medium as in Paper I, i.e. two homogeneous isotropic perfectly elastic halfspaces in a welded contact along a plane interface. The method of Gaussian beams used for computations is explained in Paper I, where all the necessary equations are given. For a more detailed description of the propagation of Gaussian beams in general two-dimensional laterally smoothly inhomogeneous media see [2, 3] and for Gaussian beams in laterally varying layered structures see [4]. For many other references on Gaussian beams we refer the reader to the above-mentioned papers.

Note that the results presented here were computed using the program written by the first named author as a part of her Diploma Thesis at the Charles University, Prague [5].

2. PARAMETERS OF COMPUTATION

There are two groups of computation parameters of reflected and transmitted waves in the Gaussian beam method in the simple model described in the introduction. The first group of parameters specifies the model, the source, the receiver and the type of wave. The results of the computations, of course, depend considerably on these parameters. The second group of parameters consists of auxiliary parameters which control the computation, such as the initial parameters of Gaussian beams, parameters of the expansion of the wave field into Gaussian beams, etc. In principle, the results of computations should not be influenced by the auxiliary parameters of the second group. However, some influence is to be expected and we must learn how to choose the parameters to obtain sufficiently accurate results. For example, it is clear that for higher frequencies it will be necessary to consider a denser system of rays.

Let us now specify in more detail the individual parameters in both groups.

The first group consists of the following parameters:

a) The parameters of the model: α_1, β_1, ϱ_1 for the first halfspace (in which the source is situated), α_2, β_2, ϱ_2 for the second halfspace. The quantities α_i and β_i denote the velocities of compressional and shear waves, respectively, ϱ_i the densities.

b) The parameters of the source: The source is situated in the first halfspace, at a distance h from the interface. A point or a line source may be considered. The frequency of the generated wave field is f (Hz).

c) The parameters of the receiver: Coordinates of the receivers are denoted by x, z. Either the vertical (U_z) or the horizontal (U_x) component of the displacement vector is computed. Similarly, the *SH* component (U_y) may be evaluated. U_z, is positive upwards, U_x to the right.

d) Parameters specifying the type of wave: Reflected waves of types *PP*, *PS*, *SP* and *SS* and the transmitted waves of the same type may be computed.

The second group consists of the parameters:

a) Parameters controlling the expansion of the wave field into Gaussian beams: The parameters φ_{MIN}, φ_{MAX}, $\Delta\varphi$ specify the minimum angle, maximum angle and the angle increment of the expansion of the wave field into Gaussian beams, see Paper I, Eq. (28).

b) Initial parameters of Gaussian beams: S_0, L_0 (in kilometers). The quantities S_0 and L_0 do not depend on the angle φ in the expansion. The quantity S_0 specifies the distance of the point where the Gaussian beam is narrowest from the source, L_0 is the minimum effective half-width of the beam for the frequency of 1 Hz. See Fig. 3 in Paper I.

c) The parameter a_0 of the windowing of Gaussian beams. The contribution of the Gaussian beam is neglected in those parts of the beam where the amplitude is a_0 − times smaller than the amplitude on the central ray. See Fig. 6 for $a_0 = 0{\cdot}1$, $0{\cdot}3$, $0{\cdot}5$ and $0{\cdot}7$.

d) The parameter controlling the evaluation of the additional component.

In this paper, we shall mainly investigate the sensitivity of the results to the auxiliary parameters of the second group. The parameters of the first group will be mostly kept fixed.

The following parameters will be fixed throughout the paper:

The parameters of the model: $\alpha_1 = 6{\cdot}4$ km/s, $\alpha_2 = 8$ km/s, $\beta_i = \alpha_i/\sqrt{3}$, $\varrho_i = 1{\cdot}7 + 0{\cdot}2\alpha_i$ $(i = 1, 2)$. These parameters correspond to a typical interface with a small velocity contrast, like a Mohorovičić discontinuity.

The parameters of the source and the receivers: Both the distances of the source and the receivers from the interface are 30 km $(h = z = 30$ km). Again, these parameters correspond approximately to the depth of the Moho. Only the vertical component of the displacement vector is considered. The epicentral distance varies from 0 to 140 km, as we are interested here in the behaviour of the wave field in the critical region. (The critical distance in our model is 80 km.) A point source with a symmetrical isotropic radiation pattern is considered in all examples, both for *P* and *S* waves (although this radiation pattern is not realistic for *S* waves). The ampli-

tudes along a unit circle surrounding the source are normalized to unity both for P and S sources.

The only parameters of the first group which are different in the various examples are the frequency and the type of wave. Three frequencies are used in different figures: $f = 4$ Hz, 10 Hz and 16 Hz. The range of the frequencies covers the typical range of frequencies used in seismic investigations of the Earth's crust. In most examples, we consider PP reflected waves. Only in Sec. 6, we also show some examples of computations for other types of reflected waves, namely of the converted reflected waves PS and SP, and of the reflected SS waves.

The auxiliary parameters of the second group change from figure to figure. The selection of these parameters is always discussed in more detail in the individual sections. In all the examples, only the principal component of the Gaussian beams is used to evaluate the wave field; the additional components are not computed. The influence of the additional components on the final wave field will be studied elsewhere.

3. INITIAL PARAMETERS OF GAUSSIAN BEAMS

In this section, we shall investigate the sensitivity of the amplitude-distance curves of PP reflected waves to the two initial parameters of Gaussian beams, L_0 and S_0. We shall first discuss the influence of L_0, and then of S_0.

3.1. The quantity L_0

It was recommended in [2] to use the "optimum" value of L_0, which minimizes the width of the Gaussian beam at the receiver point for $S_0 = 0$, for computations. In our notation, for PP reflected waves, this optimum value of L_0 is given by the relation $L_0^{\text{opt}} = (2\alpha_1 D/\omega_0)^{1/2}$, where $\omega_0 = 2\pi\ \text{s}^{-1}$, and D is the distance of the receiver from the imaginary source. This yields $L_0 \sim 11-18$ km for the range of epicentral distances from 0 to 140 km. In comparisons with the exact computations, however, better agreement was obtained for higher values of L_0. For example, it was shown in Fig. 9 of Paper I that for $L_0 \sim 70$ km the coincidence of the results obtained with Gaussian beams with the exact solutions was practically perfect. We can thus consider the amplitude-distance curves computed for such high values of L_0 as exact, and investigate how the results will change when we take L_0 to be smaller. We shall consider L_0 in the range from ~ 10 km to 70 km. We shall select two typical values of L_0, for which we shall present the results in more detail: $L_0 = 28{\cdot}5$ km and $L_0 = 71{\cdot}5$ km.

In the computations, the quantity $\bar{L}_0 = (\omega_0/2\alpha_1)^{1/2} L_0$ was used instead of L_0. The values of $L_0 = 28{\cdot}5$ km and $71{\cdot}5$ km correspond to $\bar{L}_0 = 20\ \text{km}^{1/2}$ and $50\ \text{km}^{1/2}$, respectively. To be consistent with other papers on Gaussian beams, we have transformed all $\bar{L}_0$ to L_0 in this paper.

In Figs. 1 and 2, we can see the amplitude-distance curves of *PP* reflected waves for three frequencies: $f = 4$ Hz, 10 Hz and 16 Hz. Figure 1 is evaluated for $L_0 = 71{\cdot}5$ km, and Fig. 2 for $L_0 = 28{\cdot}5$ km. For comparison, the dashed curves represent the ray amplitude-distance curves. In the figures, we can observe a well-known

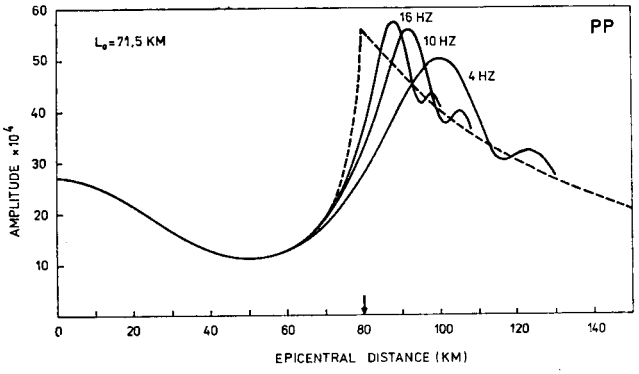

Fig. 1. The amplitude-distance curves of *PP* waves reflected from a plane interface evaluated by the Gaussian beam method, for the frequencies $f = 4$ Hz, 10 Hz and 16 Hz. The ray amplitude distance curve (dashed line) is shown for comparison. Parameters of computation: $L_0 = 71{\cdot}5$ km, $S_0 = 0$ km, $a_0 = 0{\cdot}1$, $\Delta\varphi = 0{\cdot}57$ degrees. The frequency-dependent behaviour of the reflected waves in the critical region can be seen distinctly.

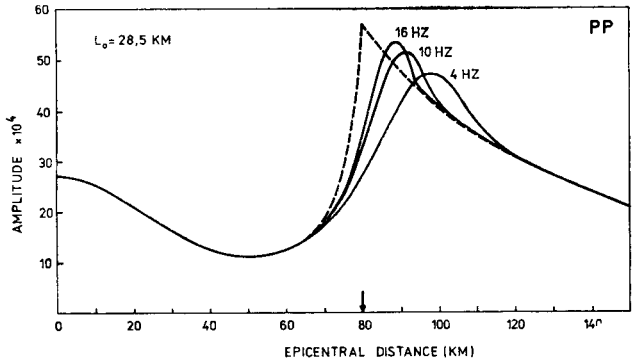

Fig. 2. The same as in Fig. 1, for $L_0 = 28{\cdot}5$ km.

effect in the critical region: the maximum of the amplitude-distance curve is shifted beyond the critical point. This effect is frequency-dependent; the shift is larger for smaller frequencies. For a detailed discussion refer to Paper I.

As we can see, the only differences between the figures computed for $L_0 = 28{\cdot}5$ km and $L_0 = 71{\cdot}5$ km are in the overcritical region, where the oscillations of the amplitude-distance curves (caused by head waves) are smoothed for the smaller value of L_0.

To emphasize the differences between the results obtained for both values of L_0,

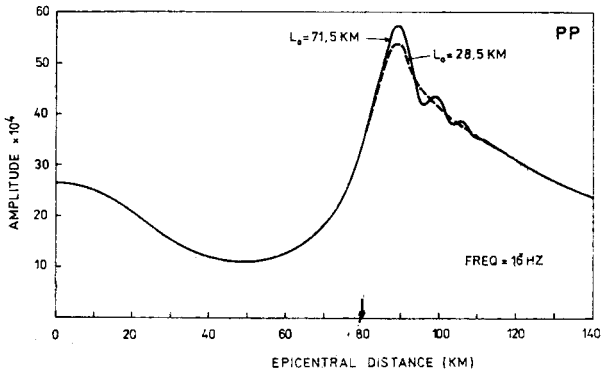

Fig. 3a. Comparison of the amplitude-distance curves of *PP* waves reflected from a plane interface evaluated by the Gaussian beam method for $L_0 = 71{\cdot}5$ km and $L_0 = 28{\cdot}5$ km. Frequency equals 16 Hz.

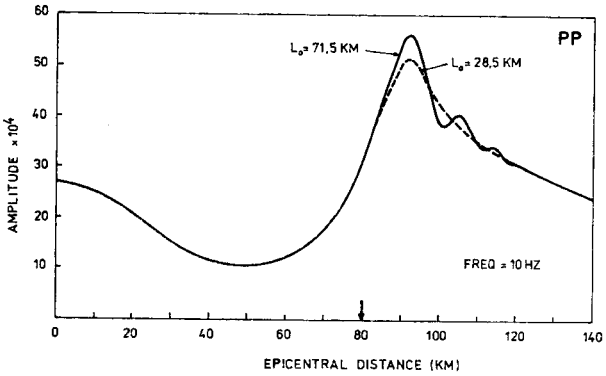

Fig. 3b. The same as in Fig. 3a, for the frequency of 10 Hz.

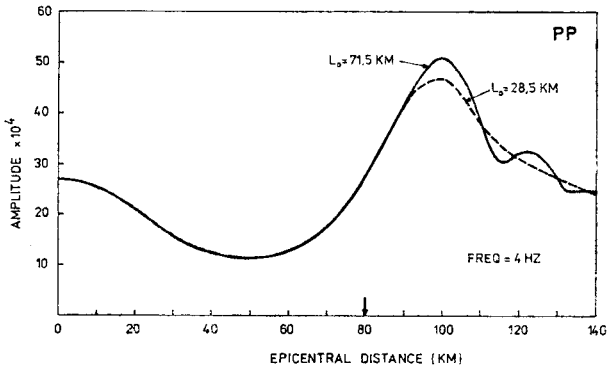

Fig. 3c. The same as in Fig. 3a, for the frequency of 4 Hz.

Figures 3a, 3b and 3c present these comparisons for the frequencies $f = 4$ Hz, 10 Hz and 16 Hz separately. The general behaviour of both curves evaluated for $L_0 = 24{\cdot}5$ km and $L_0 = 71{\cdot}5$ km is very similar in all three cases. At subcritical distances, the results practically coincide. In the critical region, in the neighbourhood of the maximum of the amplitude-distance curve, the amplitudes for $L_0 = 28{\cdot}5$ km are smaller than those for $L_0 = 71{\cdot}5$ km. The differences are, however, less than 10%. In the overcritical distance, the curve for $L_0 = 28{\cdot}5$ km is a smoothed average of the exact amplitude curve.

In Fig. 4, the amplitudes versus L_0 at epicentral distances of 0, 70, 80, 90, 100, 150 km are shown for the frequency of 16 Hz. As we can see in Fig. 3a, the epicentral distance of 90 km corresponds approximately to the maximum of the amplitude-distance curve, where the influence of L_0 is the largest.

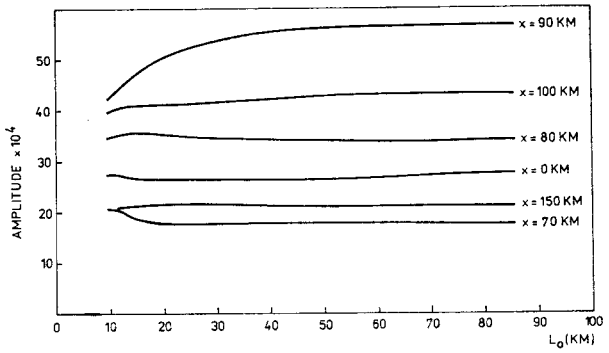

Fig. 4. The amplitudes of *PP* waves reflected from a plane interface evaluated by the Gaussian beam method versus L_0, for the frequency of 16 Hz and for various epicentral distances x. Other parameters of computation: $S_0 = 0$ km, $a_0 = 0{\cdot}1$, $\Delta\varphi = 0{\cdot}57$ degrees. Only at epicentral distances close to 90 km, where the amplitude-distance curve has a maximum, can a more pronounced influence of L_0 on amplitudes be observed.

The general results following from Fig. 4 and from other similar figures not presented here are as follows. The amplitudes are more influenced by the choice of L_0 only in the region close to the maximum of the amplitude-distance curves. The position of the maximum, however, is very stable, it practically does not depend on the choice of parameters. Only the level of amplitudes in this region depends on L_0. In the frequency range from $f = 4$ Hz to 16 Hz, for L_0 larger or equal to the optimum value, the maximum difference may even reach 20%. For L_0 larger than 40, the difference is less than 2% at any epicentral distance; for L_0 larger than 30 the difference is less than 7%. If we exclude the epicentral distances close to the maximum of the amplitude-distance curve, the results are practically independent of L_0 in a broad range of L_0.

3.2. The quantity S_0

Many test computations with various S_0 were performed. Generally, when L_0 is not too small (say, $L_0 > 20$ km) the results are practically not influenced by S_0. Figure 5 shows the amplitude-distance curves for $f = 4$ Hz and for $L_0 = 71{\cdot}5$ km and $S_0 = 0$ km (by a continuous line). The dots denote the computed values for

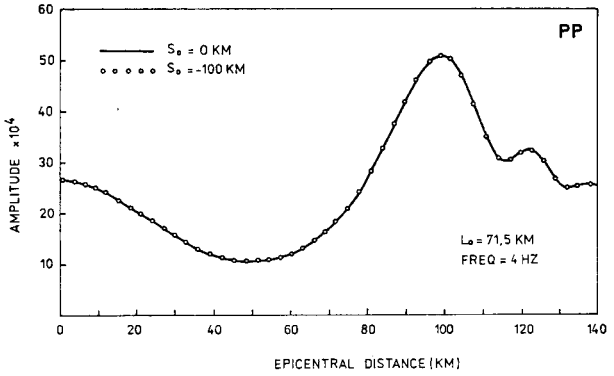

Fig. 5. The amplitude-distance curve of *PP* wave reflected from a plane interface evaluated by the Gaussian beam method, for the frequency of 4 Hz and for two values of S_0 : $S_0 = 0$ km and $S_0 = -100$ km. The continuous line corresponds to $S_0 = 0$ km, the dots to $S_0 = -100$ km. Note that the same results were obtained even for $S_0 = 100$ km. Other parameters of comp utation: $L_0 = 71{\cdot}5$ km, $a_0 = 0{\cdot}1$, $\Delta\varphi = 0{\cdot}57$ degrees.

$S_0 = -100$ km. The same values were computed for $S_0 = 100$ km, but they fully coincide with the dots for $S_0 = -100$ km. The coincidence is very good even in the critical and overcritical distances.

Similar results were obtained even for other frequencies.

The influence of S_0 is more distinct only for very small L_0 (say, $L_0 \sim 5$ km). Such small L_0 are, however, not considered in this paper.

4. THE WINDOWING OF GAUSSIAN BEAMS

The windowing of Gaussian beams (see Sec. 3.2 in Paper I) is controlled by the quantity a_0. The windowed Gaussian beams for $a_0 = 0{\cdot}1, 0{\cdot}3, 0{\cdot}5$ and $0{\cdot}7$ are showed in Fig. 6.

Figures 7 and 8 compare the results obtained with $a_0 = 0{\cdot}1$ and $0{\cdot}5$, for frequencies $f = 4$ Hz and 16 Hz and for $L_0 = 71{\cdot}5$ km. The continuous lines correspond to $a_0 = 0{\cdot}1$ and the dots to $a_0 = 0{\cdot}5$. As we can see, even the robust windowing ($a_0 = 0{\cdot}5$) does not change the character of the amplitude-distance curve, even though it yields in some cases, a little larger local differences. The differences between the results obtained for $a_0 = 0{\cdot}1$ and $0{\cdot}5$ are not systematic, in some regions the ampli-

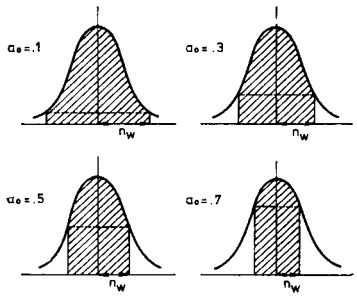

Fig. 6. The windowing of Gaussian beams for four values of a_0: 0·1, 0·3, 0·5 and 0·7. Only the hatched parts of Gaussian beams are used in the computations. The half-width of the window is denoted by n_w.

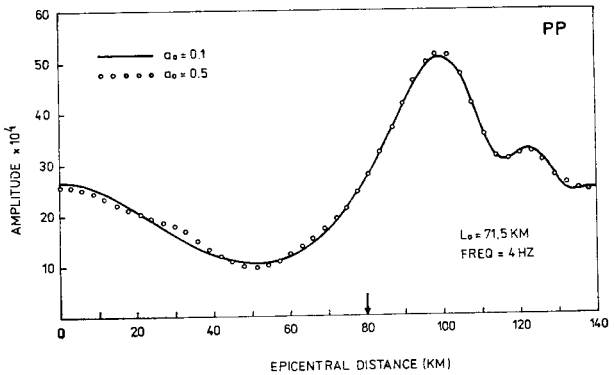

Fig. 7. The amplitude-distance curves of *PP* waves reflected at a plane interface evaluated by the Gaussian beam method for the frequency of 4 Hz and for two values of a_0 : $a_0 = 0{\cdot}1$ and 0·5. The continuous line corresponds to $a_0 = 0{\cdot}1$, the dots to $a_0 = 0{\cdot}5$. Other parameters of computation: $L_0 = 71{\cdot}5$ km, $S_0 = 0$ km, $\Delta\varphi = 0{\cdot}57$ degrees. Even robust windowing ($a_0 = 0{\cdot}5$) yields results satisfactory from a practical point of view.

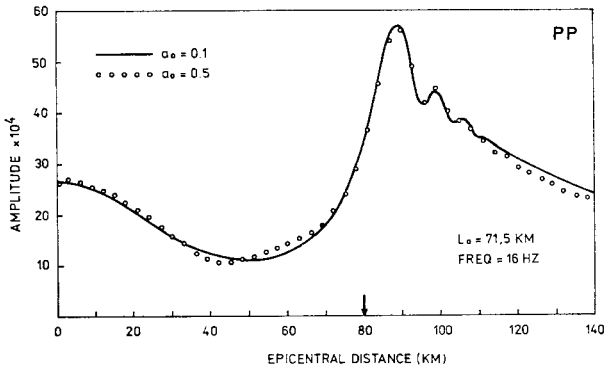

Fig. 8. The same as in Fig. 7, for the frequency of 16 Hz. The influence of a_0 is slightly larger than for the frequency of 4 Hz.

tudes obtained by robust windowing are larger and in other smaller than the exact values.

In Fig. 9, amplitudes versus a_0 for several epicentral distances are shown, for $f = 4$ Hz and $L_0 = 28{\cdot}5$ km. Even though the curves show some variations, mainly

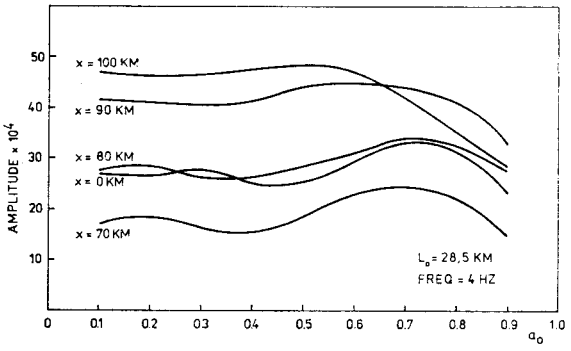

Fig. 9. The amplitudes of *PP* waves reflected from a plane interface evaluated by the Gaussian beam method for the frequency of 4 Hz versus a_0. The numbers at the curves denote the epicentral distances. Other parameters of computation: $L_0 = 28{\cdot}5$ km, $S_0 = 0$ km, $\Delta\varphi = 0{\cdot}57$ degrees.

for $a_0 > 0{\cdot}4$, it is very surprizing to see that even for $a_0 = 0{\cdot}9$ the results are not completely destroyed. Only the curve for the epicentral distance of 100 km, where the maximum of the amplitude-distance curve is situated, shows a fast decrease of amplitudes with increasing a_0 larger than $0{\cdot}6$.

The reason why the robust windowing of Gaussian beams can be used is in the destructive interference of remote Gaussian beams. The effect of Gaussian decrease of amplitudes perpendicular to the central ray is combined with the effect of the curvature of the phase fronts of Gaussian beams, which leads to the destructive interference of the parts of Gaussian beams remote from the central ray. Only the central parts of Gaussian beams play an important role in the summation of the beams.

5. THE PARAMETERS CONTROLLING THE EXPANSION OF THE WAVE FIELD INTO GAUSSIAN BEAMS

The expansion of the wave field into Gaussian beams is controlled by the three parameters φ_{MIN}, φ_{MAX} and $\Delta\varphi$. To some extent, the parameters φ_{MIN} and φ_{MAX} only have a formal meaning as the width of the cone of rays used for computations is controlled automatically by the windowing parameter a_0. As the influence of a_0 on the results was discussed in the preceding section, we shall now mainly discuss the influence of the density of the rays on the results.

In Figs. 10a–c, the amplitudes versus $\Delta\varphi$ for several epicentral distances and for frequencies $f = 4$ Hz, 10 Hz and 16 Hz are shown. The numbers near the individual points of these curves show the number of Gaussian beams used to construct the wave field. (This number is automatically controlled by the quantity a_0). All the figu-

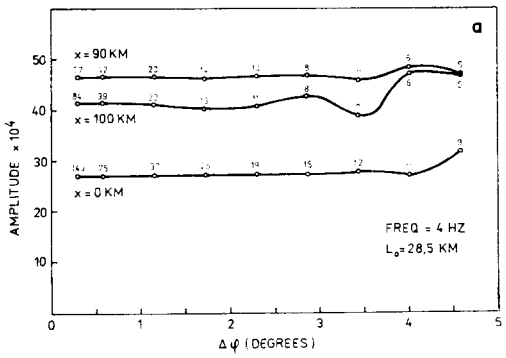

Fig. 10a. The amplitudes of *PP* waves reflected from a plane interface evaluated by the Gaussian beam method, for frequency of 4 Hz, versus $\Delta\varphi$ (the step in the initial angles of the rays). The numbers at the small circles denote the number of Gaussian beams automatically used for the evaluation of the wave field. Other parameters of computation: $L_0 = 28{\cdot}5$ km, $S_0 = 0$ km, $a_0 = 0{\cdot}1$. It is sufficient to use $\Delta\varphi \sim 3$ degrees for frequencies close to 4 Hz.

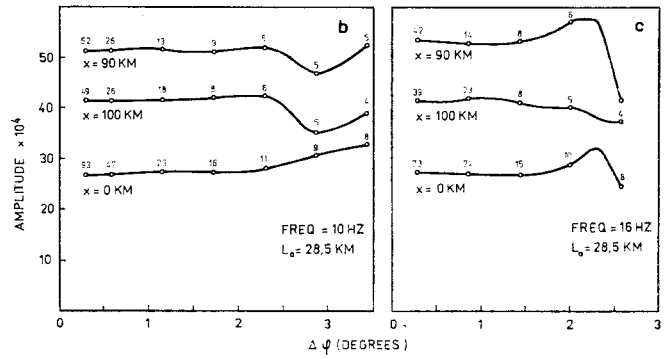

Fig. 10b. The same as in Fig. 10a, for the frequency of 10 Hz.

Fig. 10c. The same as in Fig. 10a, for the frequency of 16 Hz. The quantity $\Delta\varphi$ must be taken to be smaller than for the frequency 4 Hz, about 1·5 degrees or less.

res clearly indicate that the integration step $\Delta\varphi$ adopted for higher frequencies must be smaller. This is quite natural. For the frequency of 4 Hz, $\Delta\varphi$ may be taken as large as ~ 3 degrees, without affecting the results. For $f = 16$ Hz, $\Delta\varphi$ should be smaller, approximately $\Delta\varphi \leqq 1{\cdot}5$ degrees.

The number of beams, used to construct the wave field, depends, of course, on a_0.

In our pictures, evaluated with $a_0 = 0{\cdot}1$, the sufficient number of beams is 6–10, depending on the epicentral distance. The number of ten Gaussian beams is quite satisfactory in all cases. In some other cases (not presented here), the wave field was evaluated with a sufficient accuracy using 2–3 Gaussian beams only.

6. REFLECTED *PS*, *SP* AND *SS* WAVES

In the preceding sections, we investigated only the *PP* reflected waves. A similar procedure based on Gaussian beams can be used to evaluate the reflected/transmitted waves of other tapes. All the necessary equations were summarized in Paper I.

Here we shall present only three figures, in which the reflected *PS*, *SP* and *SS* waves are shown for three frequencies; $f = 4$ Hz, 10 Hz and 16 Hz. For comparison, the ray amplitude-distance curve is shown by a dashed line in all there figures. We are now only interested in the general behaviour of the amplitude-distance curves and, consequently, we take the quantity L_0 to be 28·5 km. This means that the oscillations of these amplitude-distance curves are smoothed and the curves represent some averages. In all the three figures, the positions of the critical points are denoted by arrows along the horizontal axis. A more detailed investigation of the properties of converted and SS reflected waves will be performed elsewhere, where the detailed character of amplitude-distance curves (including head waves) will be discussed.

6.1. *PS* Reflected Waves

The amplitude-distance curves of the vertical component of *PS* reflected waves are shown in Fig. 11. The amplitudes are relatively small, and only at distances of 60–70 km are they close to the amplitudes of *PP* reflected waves. The critical

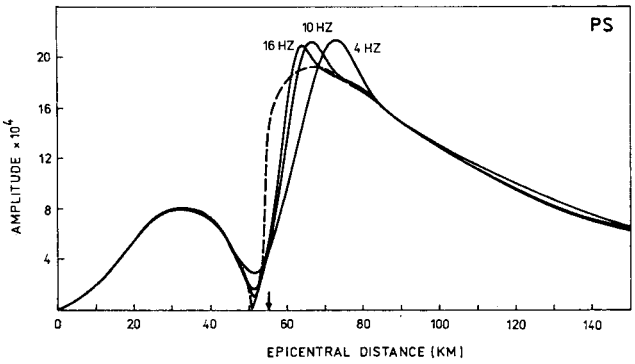

Fig. 11. The amplitude-distance curves of converted *PS* reflected wave (vertical component) evaluated for three frequencies, 4 Hz, 10 Hz and 16 Hz. The ray amplitude-distance curve (dashed line) is shown for comparison. Parameters of computation: $L_0 = 28{\cdot}5$ km, $a_0 = 0{\cdot}1$, $S_0 = 0$ km, $\Delta\varphi = 0{\cdot}57$ degrees.

point is situated at an epicentral distance of 55·6 km. The amplitude-distance curve does not have a cusp there, but an inflexion point with an infinite derivative. At overcritical distances, a similar maximum is formed on the amplitude-distance curve as in the case of *PP* reflected waves. The position of the maximum is again frequency-dependent. At an epicentral distance of 51 km, the ray amplitudes vanish and the ray-amplitude-distance curve has a sharp spike there. The Gaussian beam method smoothes this spike. Again, the smoothing is frequency-dependent.

6.2. *SS* Reflected Waves

The amplitude-distance curves of the vertical component of the *SS* reflected waves are shown in Fig. 12. As is well known, three critical regions are formed in the *SS* reflected wave field. At small epicentral distances, the amplitudes are relatively small.

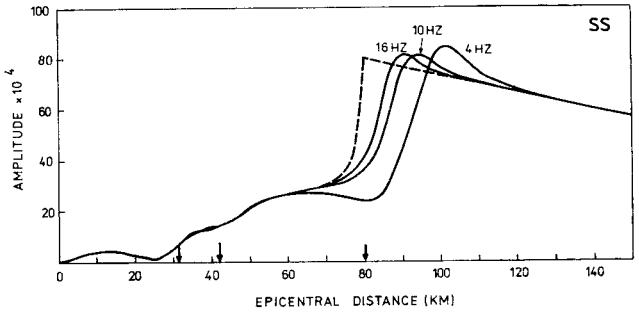

Fig. 12. The amplitude-distance curves of *SS* reflected waves (vertical component) evaluated by the Gaussian beam method. All parameters of computation are the same as in Fig. 11.

This is mainly due to the fact that we are considering the vertical component here; and the ray of the *SS* wave is nearly vertical at small epicentral distances. Only at epicentral distances beyond 80 km are the amplitudes considerably higher. At this region, they are even stronger than those of *PP* reflected waves. The displacement of the maximum of the amplitude-distance curve is again frequency-dependent and slightly larger than the displacement of the maximum of the *PP* reflected wave.

6.3. *SP* Reflected Waves

The amplitude-distance curves of the vertical component of the *SP* reflected waves are shown in Fig. 13. The amplitudes are very small in comparison with those of *PP*, *PS* and *SS* waves. The critical point is again situated at an epicentral distance of 55·6 km as in the case of *PS* waves. At subcritical epicentral distances, the behaviour of the curves is very similar to that of *PS* waves. At overcritical epicentral distances, they are also similar to those of *PS* waves, but they are about 3 times

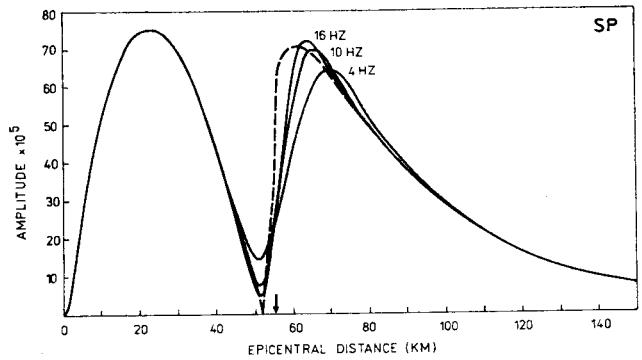

Fig. 13. The amplitude-distance curves of converted *SP* reflected waves (vertical component) evaluated by the Gaussian beam method. All parameters of computations are the same as in Fig. 11.

weaker. At epicentral distances close to 40 km, the amplitudes of *SP* reflected waves are only slightly smaller than the amplitudes of *PP* reflected waves (assuming the same normalization of *P* and *S* sources).

7. CONCLUSIONS

Let us summarize the most important results obtained in this paper and in its first part, Paper I. In both these papers, the Gaussian beam method was used to analyze the time-harmonic field of waves reflected from a plane interface with a small velocity contrast. The main purpose was to investigate the accuracy of the method of Gaussian beams and its sensitivity to certain auxiliary parameters used in the computations, such as the initial parameters of Gaussian beams. The main results for the *PP* reflected wave field are as follows:

a) The method of Gaussian beams yields sufficiently accurate results for the *PP* reflected wave field, even in the singular critical region.

b) In the subcritical region, the results are very stable, practically independent of the choice of auxiliary parameters.

c) In the critical region, the amplitude-distance curve of the reflected wave has a maximum, which is displaced beyond the critical point. The displacement is frequency-dependent. The method of Gaussian beams is capable of determining the position of the maximum with very high accuracy. The position of the maximum is practically independent of the auxiliary parameters adopted.

d) In the critical region, the most accurate results are obtained for high L_0 (the minimum half-width of the Gaussian beam). For smaller L_0, a less pronounced maximum is obtained (although the position of the maximum is not influenced by the change of L_0).

e) In the overcritical region, the amplitudes of reflected waves generally depend

only slightly on the choice of L_0. For high L_0, an oscillatory amplitude-distance curve is obtained; the oscillations being due to head waves. The head waves are thus obtained automatically by the summation of the reflected Gaussian beams. For lower L_0, however, the oscillations vanish and a smoothed average is obtained. This means that the head waves are not obtained in this case (see [6]).

f) The second initial parameter of the Gaussian beams, S_0 (which represents the distance between the source and the place where the Gaussian beam is narrowest, measured along the ray), has practically no influence on the amplitude-distance curves (when L_0 is not small) and may be chosen arbitrarily. The simplest way is to put it equal to zero.

g) The windowing of the Gaussian beams has only slight influence on the amplitude-distance curves of reflected waves. Even a very robust windowing in which only a narrow central part of the Gaussian beam is considered, yields results of satisfactory accuracy at all epicentral distances, including the singular critical region.

h) The density of the rays used to construct the expansion of the wave field into Gaussian beams depends, of course, on the frequency. For frequencies close to 4 Hz, it was sufficient to take $\Delta\varphi$ (the step in the initial angle of the ray in the expansion) as large as 3 degrees. For a frequency of 16 Hz, it was necessary to take $\Delta\varphi$ to be about 1·5 degrees or less.

i) It is not necessary to consider too many Gaussian beams in the summation. To obtain the amplitudes with a sufficient accuracy at any point in the medium, only about 6–10 Gaussian beams passing in the neighbourhood of the receiver need be considered. In robust modelling, 3–5 Gaussian beams usually yield reliable results.

The method of Gaussian beams can also be used without any problem to evaluate the wave field of converted *PS* ansd *SP* waves, and of *SS* reflected/transmitted waves. Examples presented in this paper again show that the method of Gaussian beams describes the various frequency-dependent effects in the wave fields of the above listed waves accurately. A more detailed investigation of these waves will be performed elsewhere.

All the conclusions listed above correspond, strictly speaking, to the model under consideration and to the investigated wave field. The authors expect that several conclusions may apply generally. Some other conclusions, however, particularly those regarding L_0 and S_0, may depend, more or less, on the model and wave fields under consideration. Other test computations and comparisons with exact solutions will have to be made to be able to draw more general conclusions.

Received 13. 5. 1983 *Reviewer: I. Pšenčík*

References

[1] J. Konopásková, V. Červený: Numerical Modelling of Time-Harmonic Seismic Wave Fields in Simple Structures by the Gaussian Beam Method, Part I. Studia geoph. et geod., 28 (1984), 19.
[2] V. Červený, M. M. Popov, I. Pšenčík: Computation of Wave Fields in Inhomogeneous Media — Gaussian Beam Approach. Geoph. J. R. Astr. Soc., 70 (1982), 109.
[3] V. Červený, I. Pšenčík: Gaussian Beams in Two-Dimensional Elastic Inhomogeneous Media. Geoph. J. R. Astr. Soc., 72 (1983), 417.
[4] V. Červený, I. Pšenčík: Gaussian Beams in Two-Dimensional Laterally Varying Layered Structures. Geoph. J. R. Astr. Soc., (submitted).
[5] J. Hronová: Výpočet vlnových polí v jednoduchých strukturách metodou gaussovských svazků. Dipl. práce, MFF UK, Praha 1982 (not published).
[6] V. Červený: Synthetic Body Wave Seismograms for Laterally Varying Layered Structures by the Gaussian Beam Method. Geophys. J. R. Astr. Soc., 73 (1983), 389.